

Mesoscale modeling of the temperature-dependent viscoelastic behavior of a Bitumen-Bound Gravels

Libasse Sow^{1,2}, Fabrice Bernard^{*1}, Siham Kamali-Bernard¹ and
Cheikh Mouhamed Fadel Kébé²

¹Laboratoire de Génie Civil et Génie Mécanique (LGCGM), INSA de Rennes, France

²Ecole Supérieure Polytechnique, Université Cheikh Anta Diop de Dakar, Sénégal

(Received December 3, 2017, Revised April 17, 2018, Accepted April 18, 2018)

Abstract. A hierarchical multi-scale modeling strategy devoted to the study of a Bitumen-Bound Gravel (BBG) is presented in this paper. More precisely, the paper investigates the temperature-dependent linear viscoelastic of the material when submitted to low deformations levels and moderate number of cycles. In such a hierarchical approach, 3D digital Representative Elementary Volumes are built and the outcomes at a scale (here, the sub-mesoscale) are used as input data at the next higher scale (here, the mesoscale). The viscoelastic behavior of the bituminous phases at each scale is taken into account by means of a generalized Maxwell model: the bulk part of the behavior is separated from the deviatoric one and bulk and shear moduli are expanded into Prony series. Furthermore, the viscoelastic phases are considered to be thermorheologically simple: time and temperature are not independent. This behavior is reproduced by the Williams-Landel-Ferry law. By means of the FE simulations of stress relaxation tests, the parameters of the various features of this temperature-dependent viscoelastic behavior are identified.

Keywords: hierarchical multi-scale modeling; road aggregates; bitumen; viscoelasticity; Prony series; thermorheological simplicity; WLF law; standardized elastic moduli; standardized volume moduli

1. Introduction

1.1 On the interest of bituminous binders in road engineering

In road engineering, the different layers must be made of materials capable of recovering and distributing loads from rolling vehicles. The foundations of pavement play an important structural role in reducing the stresses on the foundation floor. The materials constitutive of these layers must have mechanical characteristics enabling them to fully perform their functions in the pavement structure. To reach such a goal, materials constitutive of the upper layers of a road structure need to be treated by a binder. Hydraulic (e.g., cement) and bituminous binders may thus be considered alone or in a combination of both of them.

The treatment with cement enables one to achieve great performances in terms of stiffness or

*Corresponding author, Associate Professor, E-mail: fabrice.bernard@insa-rennes.fr

resistance but as any other cementitious materials, this kind of road materials are also characterized by their brittleness and their sensitivity to cracking, whatever is the cause of this cracking.

The use of bituminous binder may decrease this particular risk but the behavior of road materials with this kind of binder needs to be accurately known in a performance-based design procedure. More especially, bituminous binders exhibit a sensitivity to temperature and their behavior passes from brittle and sensitive to cracking at low temperatures to very soft and then sensitive to pavement deformation at high temperatures.

1.2 On the interest of morphological multi-scale simulations for heterogeneous materials

These last years, bituminous road materials and pavement technology have experienced a fundamental innovative transition and their study changes from an empirical approach to a mechanistic engineering one. This transition process is firstly the consequence of increasing performances requirements especially in terms of bearing capacity, durability and repair possibilities. The main objective now is to propose to the materials developers a rational approach and also to assist the structural mechanical engineers by providing tools enabling them to introduce fundamental and accurate materials behaviors.

In the same time, since now 10 years, there has been a tremendous increase in multiscale modeling investigation of the behavior of building and construction materials (Wittman 2008, Van Breugel 2008). It is well recognized now that the development of computational strategies to predict the mechanical properties of this kind of materials is of undeniable practical importance and that these strategies need to be based on a realistic and multi-scale description of the materials structure. Indeed, construction materials are inherently heterogeneous. Furthermore, the large differences between the mechanical properties of the various constituents of the materials increase even more their heterogeneity. These heterogeneous materials are preferential sites of damage and rupture, due in part to stress concentrations in certain phases or to certain interfaces and, on the other hand, to a possible decrease in fracture properties on or near interfaces or interphases.

However, the structure is thus too complex and random to allow for the development of analytical schemes enabling one to link the properties to the structure. This is where simulation based investigations could make the difference, using the advanced numerical tools available today. More particularly, simulations have to take into account as many as possible the heterogeneities of the material structures. Studied materials need to be considered as multi-phases composites in the simulation procedure.

Several authors have thus been interested in such a modeling for non-cohesive (see for example among the most recent studies: She *et al.* 2018, Asadi *et al.* 2018, Zhu *et al.* 2016) as well as for cohesive granular materials (Narayan *et al.* 2017, Iona *et al.* 2017, Yang *et al.* 2017, Brahim *et al.* 2017, Želiko and Joško 2017, Hadi and Vahab 2016, Eyad *et al.* 2016, Wei *et al.* 2016, Augusto and Ki 2015, She *et al.* 2014, Saliba *et al.* 2013, Schlangen *et al.* 2009, Grondin *et al.* 2007) including some co-authors of this present work (Bernard *et al.* 2008, 2010, 2012, 2015, Kamali-Bernard *et al.* 2009a, 2009b, 2011, 2014, Comby-Peyrot *et al.* 2009, Keinde *et al.* 2014, Fu *et al.* 2017a, 2017b). These last studies were generally devoted to concrete materials and very few works were performed on road materials, at the exception of (Allou *et al.* 2015, Tehrani *et al.* 2013a, 2013b).

It is possible to define several scales of heterogeneities for road materials treated by cement

because of the intrinsic heterogeneity of the binder, the Hardened Cement Paste (HCP). However, in comparison with HCP, bituminous binders are quite homogenous, except maybe the presence of porosity. Thus, the mesoscale appears as the pertinent level to investigate the properties of road materials treated with bituminous binder. These materials may be considered as a two phases composite material: aggregates embedded in a homogeneous matrix.

During their service life, road materials may exhibit several kinds of mechanical behavior in function of the intensity and the number of applied cycles of the loadings (Di Benedetto 1990, Ambassa 2013). The work related in this paper is devoted to the determination of the temperature-dependent linear viscoelastic behavior of road materials which is involved for low deformation values ($\mathcal{E}_{\max} \leq 10^{-4}$) and moderate number of cycles by means of a 3D mesoscale modeling approach. Starting from the behavior of a bituminous binder found in the literature, the temperature-dependent viscoelastic behavior of a given Bituminous-Bound Gravel (BBG) is determined.

2. General modeling procedure

2.1 Construction of representative elementary volumes (REV)

A bound gravel with a bitumen mass percentage of 5% is considered in the following. The particles size distribution (PSD) considered in this modeling enables the studied virtual material to correspond to the specification of aggregates that can be used in road pavements. The mean grain size curve for road aggregates is indeed considered. This size distribution is so spread that it is necessary, to avoid a too large number of particles to generate, to make an assumption of scales separation. The PSD is divided into two parts. Two scales are thus defined. The first one, namely the sub-mesoscale, contains the 0-6 mm fraction of the PSD embedded in a matrix of bitumen. The material representative of this scale is called hereafter the micro bitumen-bound gravel (μ -BBG). The second one is the mesoscale itself. It represents the bitumen-bound gravel (BBG) and is composed of the 6-25 mm fraction of the PSD embedded in the homogenous μ -BBG.

The hierarchical multi-scale modeling, which is developed in this work, consists of representing the heterogeneities of the BBG in 3D numerical Representative Element Volumes (REV) of the two defined scales. The importance to perform a 3D modeling instead of a 2D one has been put into evidence in (Sow 2018) following also the previous works of (She *et al.* 2014) or (Schlangen *et al.* 2009). The objective is to set up a methodology for the determination by simple numerical simulations of the temperature-dependent viscoelastic behavior of the BBG. For the generation of the two REV, the same procedure, as in some of the previous references of the authors (see just above), is consider to randomly generate the various aggregates in a computational voxelized volume. A “take and place” algorithm is used and grains are randomly placed in the computational volume in order from the largest one to the smallest in size. The REV volume is $40 \times 40 \times 40$ voxels in each case with a resolution of 1 mm and 2.5 mm for the μ -BBG and the BBG respectively. That corresponds to a cube of 40 mm and 100 mm on a side, respectively. The particles size distribution is divided into 3 diameters at the sub-mesoscale (μ -BBG) and 4 at the mesoscale (BBG). Tables 1 and 2 present the composition of the sub-mesoscale and the mesoscale respectively. It is worth noting that a special attention is paid to respect a REV side-to-maximal diameter ratio larger than 4, as prescribed by (Keinde 2014).

Table 1 Volume composition of the sub-mesoscopic REV: Micro Bitumen-Bound Gravel

<i>Phases</i>	<i>Volume fraction</i>
Porous bitumen	15%
Granular skeleton (0/6 mm fraction)	85%
Including:	
$\phi = 1$ mm	40%
$\phi = 3$ mm	31%
$\phi = 5$ mm	14%

Table 2 Composition of the mesoscopic REV: Bitumen-Bound Gravel

<i>Phases</i>	<i>Volume fraction</i>
Homogenous μ -BBG	47.5%
Granular skeleton (6/25 mm fraction)	52.5%
Including:	
$\phi = 07.5$ mm	22%
$\phi = 12.5$ mm	14.5%
$\phi = 17.5$ mm	11%
$\phi = 22.5$ mm	5%

Furthermore, it is also important to point out the fact that the granular skeleton represents also 85% in volume of the REV at the sub-mesoscale. Such a computational volume is only reachable by considering the smallest particles with a non-spherical shape (here, a cubic one). On the contrary, particles with larger diameter are assumed to be spherical and this shape is voxelized.

Figs. 2(a) and (b) show cross-sections of the REV obtained at the two scales.

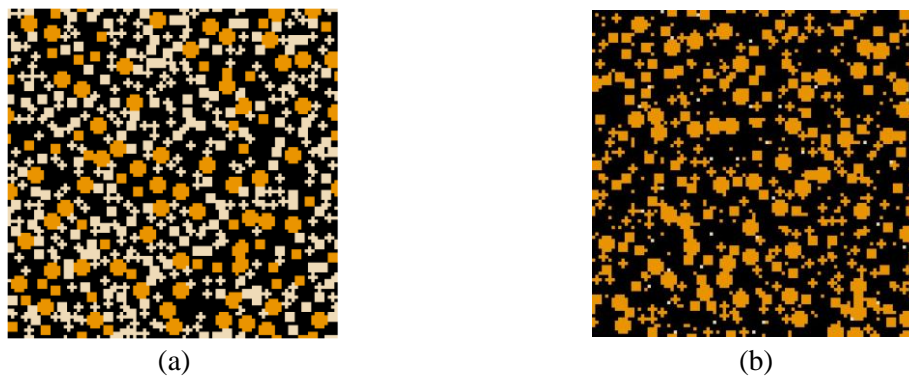


Fig. 2 Cross-section of the sub-mesoscopic REV (a) and the mesoscopic REV (b) generated with the “Take and place” method

2.2 Assumptions on the mechanical behaviors of the 2 phases at each scale

The mechanical behavior of the viscoelastic phases (bitumen and μ -BBG) at each scale is first taken into account in terms of stress relaxation by means of a generalized Maxwell model. The

bulk part of the behavior is separated from the deviatoric one and bulk and shear moduli are expanded into Prony series

$$G_R(t) = G_0 \left(1 - \sum_{k=1}^N \bar{g}_k^p (1 - e^{-t/\tau_k}) \right) \quad (1)$$

$$K_R(t) = K_0 \left(1 - \sum_{k=1}^N \bar{k}_k^p (1 - e^{-t/\tau_k}) \right) \quad (2)$$

where:

- G_0 and K_0 are respectively the instantaneous shear and bulk moduli;
- \bar{g}_k^p and \bar{k}_k^p are respectively the standardized shear and bulk moduli;
- τ_k is the relaxation time

These expressions show that the behavior of the material can be phenomenologically reproduced by parallel associations of springs and damping in series.

Furthermore, the bitumen exhibits a thermorheologically simple behavior. This principle of time-temperature equivalence makes it possible to specify the temperature dependence of the linear viscoelastic quantities. If a constant deformation is imposed at two temperatures T and T_0 , the stress relaxes faster at the highest test temperature. However, the thermorheological simplicity feature leads to consider that time and temperature are not independent state variables. The relaxation functions at two different temperatures have the same form and are only translated along the temperature scale. It implies that knowing the bituminous material behavior at a reference temperature enables one to know its behavior at any other temperature. For that, a reduced time, ξ , is introduced thanks to a shift factor $a_{T_0 \rightarrow T}(T)$

$$\log a_{T_0 \rightarrow T}(T) = - \frac{C_1(T - T_0)}{C_2 + (T - T_0)} \quad (3)$$

where T_0 is the reference temperature at which the parameters of the Prony series for both bulk and shear moduli are known. C_1 (in $^{\circ}\text{C}^{-1}$) and C_2 (in $^{\circ}\text{C}$) are two constant parameters that need to be calibrated.

2.3 Modeling strategy

In a hierarchical multi-scale modeling, such as the one developed in this paper, the outcomes at a given scale are used as input data at the next higher scale. Thus, the simulation strategy adopted in this work is summarized in Fig. 4. Stress relaxation is one of the experimental methods to study linear viscoelasticity, together with creep and dynamic techniques. Relaxation is a non-instantaneous property: when a deformation step is imposed, due to the viscoelastic behavior of the material, the material gradually returns to a more stable state, involving thus a decrease of the consecutive stress from its instantaneous to its final value. In this paper, stress relaxation is simulated by imposing a compression displacement on one of the faces of the REV. Displacements are prevented on the opposite face, the other faces are left free as shown in Fig. 3.

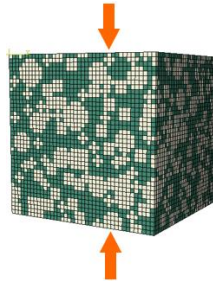


Fig. 3 Boundary conditions for stress relaxation in uniaxial compression

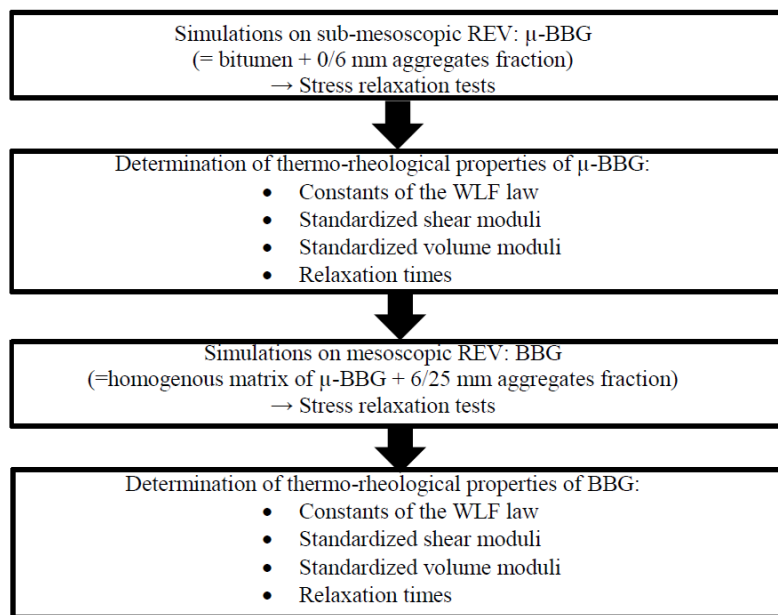


Fig. 4 Developed modeling strategy used in the hierarchical approach

The hierarchical strategy needs to define, as a starting point, each term of the Prony series of the viscoelastic phases at the sub-mesoscale and for the reference temperature: the bituminous binder. The stress relaxation 1D test at a reference temperature is simulated on a REV of the μ -BBG. The evolutions of the stress and the Young's modulus according to time may then be determined. Thanks to the well-known relationships between shear and bulk moduli with Young's modulus (Eqs. (4) and (5)) and the definition of the Poisson ratio (Eq. (6)) that may also be determined as outcome data of the sub-mesoscale, the evolutions of G and K, or the dimensionless moduli g and k , of the μ -BBG at the reference temperature, may be drawn.

$$G_R(t) = \frac{E}{2(1 + \nu)} \tag{4}$$

$$K_R(t) = \frac{E}{3(1 - 2\nu)} \tag{5}$$

$$v(t) = \frac{(l_0 - l)/l_0}{(L_0 - L)/L_0} \tag{6}$$

where:

- l_0 and L_0 are respectively the transverse initial side length and the initial longitudinal side length of the REV;
- l and L are respectively the transverse final side length and the final longitudinal side length of the REV.

The specification of the evolution of the normalized shear and bulk moduli may be done by the specification of the shear and volumetric test data. A separate nonlinear least-squares fit may then be performed on each data set and two derived sets of Prony series parameters may be obtained at the reference temperature.

The study of the influence of the temperature needs first to define, besides the parameters of the Prony series, the two constants C_1 and C_2 of the thermorheologically simple feature WLF law for the bituminous binder. Then, after performing relaxation tests at various temperatures, the translation of the various obtained relaxation curves in order to superimpose them with the reference temperature enables one to determine the shift factor $a_{T \rightarrow T_0}$ in function of the temperature, as presented in Fig. 5. The calibration of the C_1 and C_2 constants of the WLF law for the homogenous μ -BBG may be done.

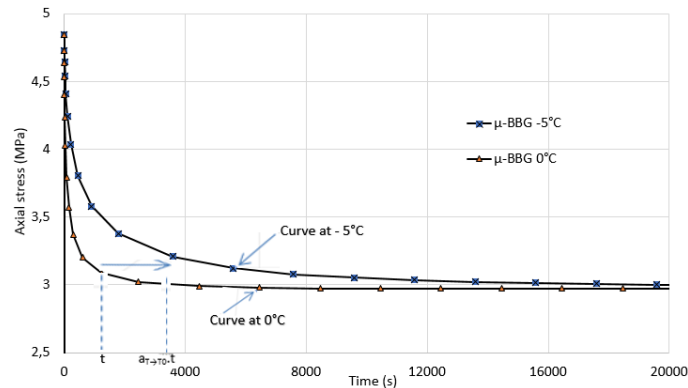


Fig. 5 Principle of test time-temperature equivalence

At the mesoscale which represents the BBG as the largest fraction of the aggregates embedded in a matrix of μ -BBG, the same simulations are performed. The input data at this scale are the outcomes at the lower scale: temperature-dependent viscoelastic behavior of the homogenous μ -BBG. The parameters of the BBG mechanical behavior are deduced in the same way than those of the μ -BBG.

3. Simulations at the sub-mesoscale: μ -BBG

3.1 Specific assumptions on the mechanical behavior of the various phases at the sub-mesoscale

The aggregates are considered to have an isotropic linear elastic behavior. The characteristics are: $E = 80$ GPa and $\nu = 0.30$.

The bituminous binder considered in this work is that studied in (Nguyen 2008) or (Tehrani 2013a). Its main characteristics are provided in these previous references. Bitumen is a viscoelastic material, that is to say that its mechanical properties depend on the duration of stress (or its frequency) and the temperature. In the isotropic linear elastic domain, the characteristics of the bitumen are the modulus of elasticity and the Poisson ratio. In his work, (Tehrani 2013a) considered a bitumen Young's modulus 37 times lower than the one of the inclusions. Based on this hypothesis, in the present modeling approach, a modulus of 2.162 GPa is imposed. In (Nguyen 2008), by adjusting experimental and numerical force-displacement curves, the Poisson ratio of the bitumen on its stretching phase has been determined. A value of 0.49 has been found. The elastic characteristics of the bitumen at the sub-mesoscopic scale are given in Table 3. The Prony series as well as the constants of the WLF law considered for the bituminous matrix are based on the work of (Nguyen 2008). The reference temperature, as defined in previous sections, is equal to 0°C.

Table 3 Isotropic elastic characteristics of the bitumen at sub-mesoscopic scale

<i>Grade of bitumen</i>	<i>E (GPa)</i>	<i>ν</i>
50/70	2.162	0.49

3.2 Results of stress relaxation tests simulations

Stress relaxation tests are simulated on the micro Bitumen-Bound Gravel. The parameters of the Prony series are obtained by a calibration using the least squares method. Contrary to the bituminous binder, very few parameters are needed to reproduce the behavior. The Prony series for the homogenous μ -BBG need two terms, as presented in Table 4.

Table 4 Prony series of the μ BBG at 0°C

<i>i</i>	<i>g_i</i>	<i>k_i</i>	<i>τ_i (s)</i>
1	0.22105	0	13.671
2	0	5.054E-02	132.05
3	0.24879	0	315.54

The stress relaxation tests are carried out at different test temperatures so as to have the same modulus for each temperature (equal to the modulus at -10°C). The stress relaxation curves at -10, -5, 0, 5 and 10°C are shown in Fig. 6. On a 4 GB RAM and 5 processors computer, the computation time for such simulations is about 1 hour.

3.3 Assessment of the thermorheologically simple parameters of the μ -BBG

From the stress relaxation curves of Fig. 6, the values of the shift factor for various temperatures may be firstly determined at the peak of each stress-time curve (time at the end of the loading phase) since the simulations have been carried out in such a way that the Young's moduli

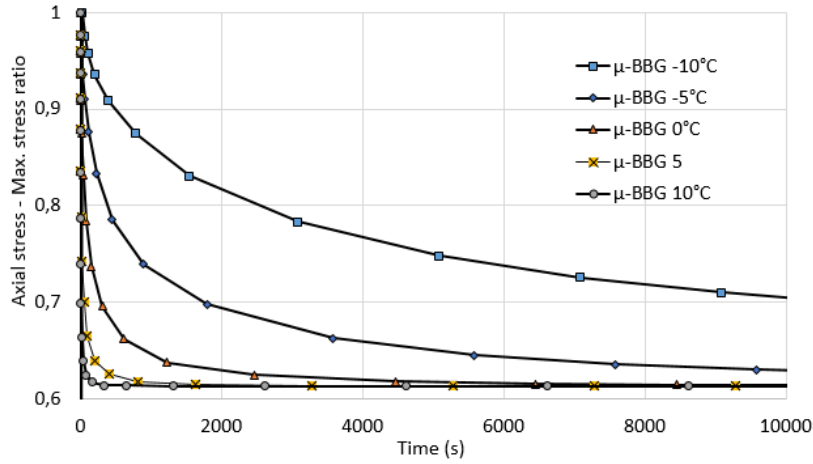


Fig. 6 Stress relaxation curves of the μ -BBG at different test temperatures

at each temperature were the same and equal to the modulus at the reference temperature (0°C). Knowing the time at the peak of each simulation for a given test temperature, the coefficient $a_{T_0 \rightarrow T}$ can be calculated according to Eq. (7). Table 5 summarizes the values of $a_{T_0 \rightarrow T}$.

$$a_{T_0 \rightarrow T} = \frac{t_{\text{peak},T}}{t_{\text{peak},T_0}} \quad (7)$$

With: $t_{\text{peak},T}$: peak time for a test temperature T ; t_{peak,T_0} : peak time for the reference temperature.

Table 5 $a_{T_0 \rightarrow T}$ values from stress relaxation simulations at different test temperatures on μ -BBG

Temperature ($^\circ\text{C}$)	$a_{T_0 \rightarrow T}$	$\log(a_{T_0 \rightarrow T})$
-10	40	1.60206
-5	5.8333	0.7659
0	1	0
5	0.1667	-0.77815
10	0.0333	-1.47712

These values of $a_{T_0 \rightarrow T}$ are used to calibrate the C_1 and C_2 constants of the WLF law. The best fit is presented in Table 6. Table 7 shows the comparisons between the values of $\log(a_{T_0 \rightarrow T})$ obtained by the simulations on the sub-meso REV and by the calibration.

Table 6 Calibrated constants of the WLF law for the μ -BBG

C_1 ($^\circ\text{C}^{-1}$)	C_2 ($^\circ\text{C}$)
20	130

Table 7 Best fit for $\log(a_{T_0 \rightarrow T}) - \mu$ -BBG

Temperature (°C)	$\log(a_{T_0 \rightarrow T})$ calculated with time at peak stress	$\log(a_{T_0 \rightarrow T})$ obtained by the WLF law with $C_1=20$ and $C_2=130$
-10	1.60205	1.6666
-5	0.76591	0.8
0	0	0
5	-0.77815	-0.74074
10	-1.47712	-1.42857

Finally, the calibration of the shift factor is validated on the whole stress-time curve. A single curve, namely the reference (or “master”) curve, is obtained as revealed by Fig. 7.

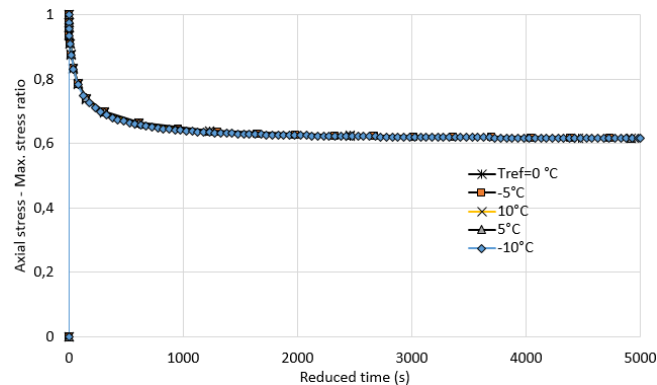


Fig. 7 Reference stress relaxation curve of the μ -BBG

4. Simulations at the mesoscale: BBG

4.1 Specific assumptions on the mechanical behavior of the various phases at the mesoscale

As at the sub-mesoscale, an isotropic linear elastic behavior is considered for the 6/25 mm fraction of the granular skeleton. Young’s modulus and Poisson ratio are respectively $E = 80$ GPa and $\nu = 0.30$.

The matrix in which the granular skeleton is embedded is composed of the micro bitumen-bound gravel seen as a homogenous phase. The behavior of this bituminous matrix is assumed to be viscoelastic. An expansion in Prony series is also considered and the parameters of this behavior are the outcomes of the previous simulations performed at the sub-mesoscale and reported in Table 4.

The constants of the WLF law used in these simulations are also those determined from the simulations performed on the μ -BBG. They are given in Table 6.

4.2 Stress relaxation tests on BBG

The stress relaxation tests are carried out at different test temperatures so as to have the same modulus for each temperature (equal to the modulus at -10°C). As a result of the simulations performed at this mesoscale, Fig. 8 shows the stress relaxation curves at -10 , -5 , 0 , 5 and 10°C . Another time, on a 4 GB RAM and 5 processors computer, the computation time for such simulations is about 1 hour.

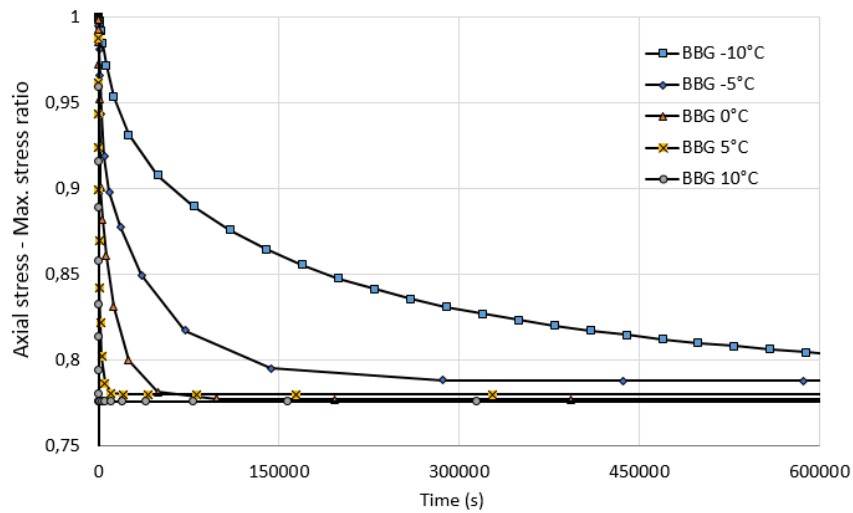


Fig. 8 Stress relaxation curves of the BBG for different test temperatures

4.3 Outcomes from stress relaxation curves

From the stress relaxation curves obtained by the simulations on the REV of BBG, the Prony series and the constants of the WLF law are determined. By calibration using a least-squares method, the Prony series of the 6/25 mm fraction of aggregates treated by bitumen may be found and the results are given in Table 8.

Table 8 Prony series of the BBG at the reference temperature of 0°C

i	g_i	ki	τ_i (s)
1	0.11265	0	16.367
2	0	2.5455E-02	124.28
3	0.14593	0	357.97

Using the same approach as in Section 3.3, the constants of the WLF law of the BBG are determined with a mean deviation of 3% for the best fit (Table 9). The parameters C_1 and C_2 of the BBG at the mesoscale have been found to be the same as for the μ -BBG (Table 10) showing that the thermorheologically simple behavior of the material at this scale is completely governed by the one of its matrix (μ -BBG). As long as they have the same constants C_1 and C_2 , the micro Bitumen-Bound Gravel and the Bitumen-Bound Gravel follow the same WLF law.

Table 9 Comparison of $\log(a_T)$ for different values of C_1 and C_2 – BBG

Temperature ($^{\circ}\text{C}$)	$\log(a_{T_0 \rightarrow T})$ calculated with time at peak stress	$\log(a_{T_0 \rightarrow T})$ obtained by the WLF law with $C_1=20$ and $C_2=130$
-10	1.60205	1.66666
-5	0.76591	0.8
0	0	0
5	-0.77815	-0.74074
10	-1.47712	-1.42856

Table 10 Calibrated constants of the WLF law for the BBG

C_1 ($^{\circ}\text{C}^{-1}$)	C_2 ($^{\circ}\text{C}$)
20	130

Finally, it is checked that with the determined shift factor, used for all temperatures and on the full-time scale, a single “master” curve is obtained (Fig. 9).

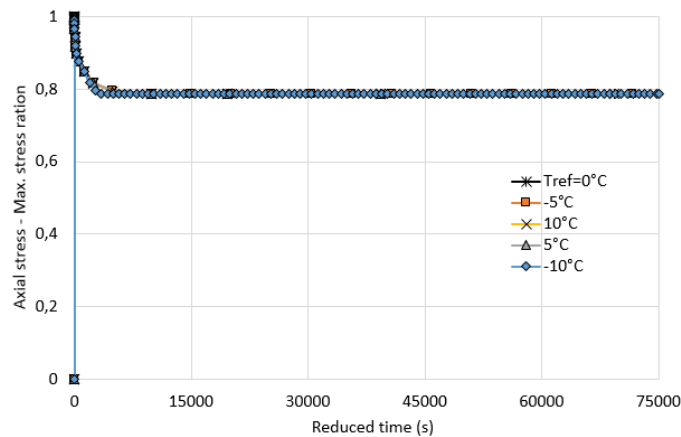


Fig. 9 Reference stress relaxation curve of the BBG

5. Validation of the temperature-dependent viscoelastic properties

In order to validate the methodology and to check the identified parameters of the temperature-dependent viscoelastic behavior, a comparison is made between the response of the heterogeneous REV and that of a homogenous REV of the same dimensions and having the characteristics obtained by the hierarchical modeling strategy. Table 11 gives the mean relative deviations between the heterogeneous and the homogenous REV responses for respectively the μ -BBG and the BBG at various temperatures. These deviations are calculated for a stress relaxation test time calibrated to be three times the time required by the mean axial stress to reach its asymptotic value. Examples of comparisons are furthermore provided in Figs. 10 and 11. It has been chosen here to present the comparisons for a temperature of $+10^{\circ}\text{C}$, where the deviation is maximal for the μ -

BBG. Some differences in the simulated test time at the sub-meso and meso-scales appear. The reason is that the μ -BBG relaxes quickly and reaches its asymptotic value for a less test time duration.

Table 11 Mean relative deviations (in %) between the responses of the homogenous and the heterogeneous REV of the μ -BBG and the BBG

Test temperature (°C)	-10	-5	0	5	10
μ -BBG	7.88	4.17	0.41	5.34	11.83
BBG	7.07	2.56	0.52	3.59	3.82

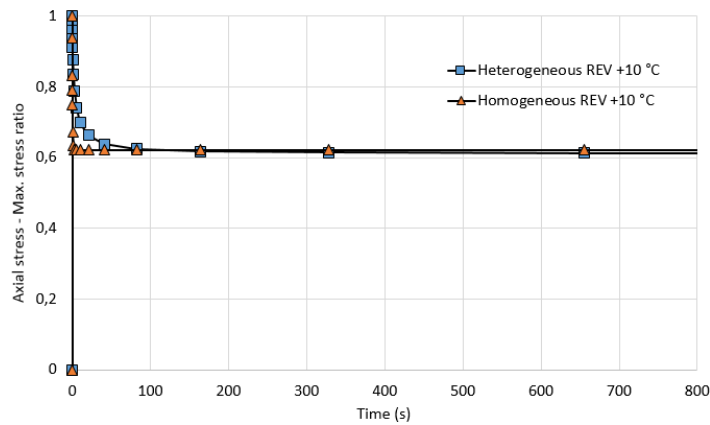


Fig. 10 Comparisons between the responses of heterogeneous and homogenous REV for μ -BBG at +10°C

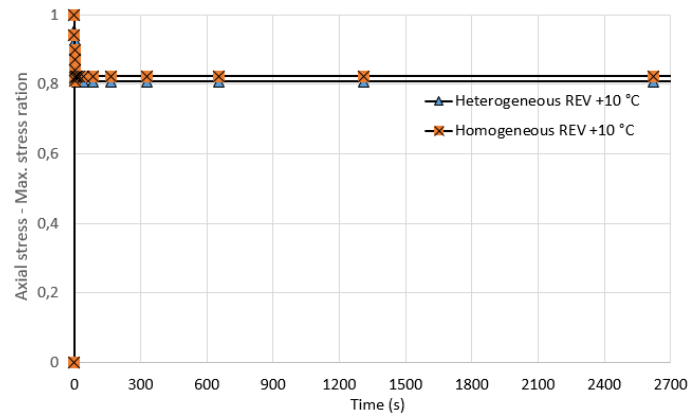


Fig. 11 Comparisons between the responses of heterogeneous and homogenous REV for BBG at +10°C

6. Conclusions

A hierarchical multi-scale modeling strategy devoted to the study of a Bitumen-Bound Gravel (BBG) is presented in this paper.

Two scales are defined in order to take into account the whole particle size distribution. At the

sub-mesoscale, the μ -BBG is defined by the smallest fraction of the PSD (0/6 mm) embedded in a matrix of bituminous binder. At the mesoscale, the BBG comprises the remaining aggregates fraction (6/25 mm) in a homogenous matrix of μ -BBG. In this hierarchical strategy, the input data for the behavior of the phases at the mesoscale are the outcomes of the simulations performed by the FE method at the sub-mesoscale.

The paper investigates the temperature-dependent linear viscoelastic of a bitumen-bound gravel that may be exhibited when the material is submitted to low deformations levels and moderate number of cycles. The viscoelastic phases at each scale are considered to follow a generalized Maxwell model and their bulk and shear moduli are expanded into Prony series. Furthermore, these viscoelastic phases are also thermorheologically simple and time and temperature are not independent. To take into account this temperature-dependent behavior, a Williams-Landel-Ferry approximation law is considered.

The parameters of the viscoelastic and thermorheologically simple behaviors for both μ -BBG and BBG are the outcomes of the developed hierarchical modeling strategy. They are identified by means of the simulation of stress relaxation tests at various temperatures. In addition, some other conclusions may be drawn:

- in comparison with the bituminous binder, the μ -BBG and BBG viscoelastic behaviors appear to be less complex since two terms of the Prony series seem to be sufficient and to describe with enough precision the behavior of these two materials;
- the thermorheologically simple behavior of the BBG is fully defined by the one of the μ -BBG and thus the two constant parameters of the WLF law are the same for each scale;
- on the contrary, the viscoelastic behavior is slightly different for each scale and the μ -BBG relaxes more quickly than the BBG.

Finally, such a multi-scale modeling approach plays the role of a “virtual laboratory” and opens numerous applications perspectives to study common problems in road engineering and several examples of pavement degradation (such as rutting, cracking...).

References

- Allou, F., Takarli, M., Dubois, F., Petit, C. and Absi, J. (2015), “Numerical finite element formulation of the 3D linear viscoelastic material model: Complex Poisson’s ratio of bituminous mixtures”, *Arch. Civil Mech. Eng.*, **15**(4), 1138-1148.
- Ambassa, Z. (2013), “Vers la modélisation du comportement à la fatigue des chaussées bitumineuses sous chargement réel”, Ph.D. Dissertation, University of Limoges, France.
- Asadi, M., Mahboubi, A. and Thoeni, K. (2018) “Discrete modeling of sand-tire mixture considering grain-scale deformability”, *Granul. Matt.*, **20**(2), 18.
- Augusto, C.F. and Ki, H.M. (2015), “Micromechanical-analogical modelling of asphalt binder and asphalt mixture creep stiffness properties at low temperature”, *Road Mater. Pavem. Des.*, **16**(1), 111-137.
- Bernard, F., Kamali-Bernard, S. and Prince, W. (2008), “3D multi-scale modelling of mechanical behavior of sound and leached mortar”, *Cement Concrete Res.*, **38**, 449-458.
- Bernard, F. and Kamali-Bernard, S. (2010), “Performance simulation and quantitative analysis of cement-based materials subjected to leaching”, *Comput. Mater. Sci.*, **50**(1), 218-226.
- Bernard, F. and Kamali-Bernard, S. (2012), “Predicting the evolution of mechanical and diffusivity properties of cement pastes and mortars for various hydration degrees-a numerical simulation investigation”, *Comput. Mater. Sci.*, **61**, 106-115.
- Bernard, F. and Kamali-Bernard, S. (2015), “Numerical study of ITZ contribution on mechanical behavior

- and diffusivity of mortars”, *Comput. Mater. Sci.*, **102**, 250-257.
- Brahim, K.V., Maryam, M.M., Abbas, R.M.R. and Gholam, H.R. (2017), “Modeling of mechanical properties of roller compacted concrete containing RHA using ANFIS”, *Comput. Concrete*, **19**(4), 435-442.
- Comby-Peyrot, I., Bernard, F., Bouchard, P.O., Bay, F. and Garcia-Diaz, E. (2009), “Development and validation of a 3D computational tool to describe concrete behaviour at mesoscale. Application to the alkali-silica reaction”, *Comput. Mater. Sci.*, **46**(4), 1163-1177.
- Di Benedetto, H. (1990), “Nouvelle approche du comportement des enrobés bitumineux: Résultats expérimentaux et formulation rhéologique”, *Proceedings of the 4th RILEM Symposium on Mechanical Tests for Bituminous Mixes, Characterization, Design and Quality Control*, Budapest.
- Eyad, M., Scarpas, A., Alieh, A., Koumbakonam, R.R. and Cor, K. (2016), “Finite element modelling of field compaction of hot mix asphalt. Part I: Theory”, *Road Mater. Pavem. Des.*, **17**(1), 13-33.
- Fu, J., Bernard, F. and Kamali-Bernard, S. (2017a), “First-principles calculations of typical anisotropic cubic and hexagonal structures and homogenized moduli estimation based on the Y-parameter: Application to CaO, MgO, CH and Calcite CaCO₃”, *J. Phys. Chem. Sol.*, **101**, 74-89.
- Fu, J., Bernard, F. and Kamali-Bernard, S. (2017b), “Assessment of the elastic properties of amorphous calcium silicates hydrates (I) and (II) structures by molecular dynamics simulation”, *Molecul. Simulat.*, In Press.
- Grondin, F., Dumontet, H., Hamida, A.B., Mounajed, G. and Boussa, H. (2007), “Multi-scales modelling for the behaviour of damaged concrete”, *Cement Concrete Res.*, **37**(10), 1453-1462.
- Hadi, H. and Vahab, S. (2016), “Numerical simulation of tensile failure of concrete using Particle Flow Code (PFC)”, *Comput. Concrete*, **18**(1), 39-51.
- Ioana, M.A., Cyrille, C., Duchez, J.L. and Saida, M. (2017), “Modelling of the fatigue damage of a geogrid-reinforced asphalt concrete”, *Road Mater. Pavem. Des.*, **18**(1), 250-262.
- Kamali-Bernard, S., Bernard, F. and Prince, W. (2009a), “Computer modelling of tritiated water diffusion test for cement-based materials”, *Comput. Mater. Sci.*, **45**(2), 528-535.
- Kamali-Bernard, S. and Bernard, F. (2009b), “Effect of tensile cracking on diffusivity of mortar: 3D numerical modelling”, *Comput. Mater. Sci.*, **47**(1), 178-185.
- Kamali-Bernard, S. and Bernard, F. (2011), “How to assess the long-term behaviour of a mortar submitted to leaching?”, *Eur. J. Environ. Civil Eng.*, **15**(7), 1031-1043.
- Kamali-Bernard, S., Keinde, D. and Bernard, F. (2014), “Effect of aggregate type on the concrete matrix/aggregates interface and its influence on the overall mechanical behavior. A numerical study”, *Key Eng. Mater.*, **617**, 14-17.
- Keinde, D. (2014), “Etude du béton à l'échelle mesoscopique: Simulation numérique et tests de micro-indentation”, Ph.D. Dissertation, INSA de Rennes.
- Keinde, D., Kamali-Bernard, S., Bernard, F. and Cisse, I. (2014), “Effect of the interfacial transition zone and the nature of the matrix-aggregate interface on the overall elastic and inelastic behaviour of concrete under compression: A 3D numerical study”, *Eur. J. Environ. Civil Eng.*, **18**(10), 1167-1176.
- Narayan, S.P.A., Little, D.N. and Rajagopal, K.R. (2016), “Modelling the nonlinear viscoelastic response of asphalt binders”, *Road Mater. Pavement Des.*, **17**(2), 123-132.
- Nguyen, H.N. (2008), “Etude numérique de la fissuration d'un milieu viscoélastique : Analyse de l'essai de rupture sur bitume”, Ph.D. Dissertation, Ecole Nationale des Ponts et Chaussée.
- Saliba, J., Grondin, F., Matallah, M., Loukili, A. and Boussa, H. (2013), “Relevance of a mesoscopic modeling for the coupling between creep and damage in concrete”, *Mech. Time-Depend. Mater.*, **17**(3), 481-499.
- Schlangen, E. and Qian, Z. (2009), “3d modeling of fracture in cement-based materials”, *J. Multisc. Modell.*, **1**(2), 245-261.
- She, W., Zhang, Y. and Jones, M.R. (2014), “Three-dimensional numerical modeling and simulation of the thermal properties of foamed concrete”, *Constr. Build. Mater.*, **50**(1), 421-431.
- She, W., Cao, X., Zhao, G., Cai, D., Jiang, J. and Hu, X. (2018), “Experimental and numerical investigation of the effect of soil type and fineness on soil frost heave behavior”, *Cold Reg. Sci. Technol.*, **148**, 148-158.

- Sow, L. (2018), "Approche couplée expérimentation-modélisation multi-échelle pour la détermination du comportement mécanique des graves routières traitées aux liants. Application à la valorisation des Mâchefers d'Incineration de Déchets Non Dangereux", Ph.D. Dissertation, INSA Rennes.
- Tehrani, F.F., Absi, J., Allou, F. and Petit, C. (2013a), "Heterogeneous numerical modelling of asphalt concrete through use of a biphasic approach: Porous matrix/inclusions", *Comput. Mater. Sci.*, **69**, 186-196.
- Tehrani, F.F., Absi, J., Allou, F. and Petit, C. (2013b), "Investigation into the impact of the use of 2D/3D digital models on the numerical calculation of the bituminous composites complex modulus", *Comput. Mater. Sci.*, **79**, 377-379.
- Van Breugel, K. (2008), "Beyond multi-scale modelling", *Proceedings of the 2nd RILEM Symposium on Concrete Modelling*, ConMod'08 Delft.
- Wei, S., Guotang, Z., Guotao, Y., Jinyang, J., Xiaoyu, C. and Yi, D. (2016), "Numerical analysis of the thermal behaviors of cellular concrete", *Comput. Concrete*, **18**(3), 319-336.
- Wittman, F. (2008), "On the development of models and their application in concrete science", *Proceedings of the 2nd RILEM Symposium on Concrete Modelling*, ConMod'08 Delft.
- Yang, K.H., Ju, H.C. and Kwon, S.J. (2017), "Modeling of chloride diffusion in concrete considering wedge-shaped single crack and steady-state condition", *Comput. Concrete*, **19**(2), 211-216.
- Željko, S. and Joško, O. (2017), "Meso scale model for fiber-reinforced-concrete: Microplane based approach", *Comput. Concrete*, **19**(4), 375-385.
- Zhu, H., Nicot, F. and Darve, F. (2016), "Meso-structure evolution in a 2D granular material during biaxial loading", *Granul. Matt.*, **18**(1), 3.